Quaternary Science Reviews 324 (2024) 108475

Contents lists available at ScienceDirect

Quaternary Science Reviews

journal homepage: www.elsevier.com/locate/quascirev

The hydraulic network of the pre-Hispanic city of Tiwanaku (Bolivia): New insights from the integration of canal morphology, hydrogeological and palaeoenvironmental data

Marc-Antoine Vella [a,b,*], Grégory Bièvre [c], Christophe Delaere [d], Julien Thiesson [e], Roger Guérin [e], Claudia Rivera-Casanovas [f], Stéphane Guédron [c,g]

[a] Institut National de Recherches Archéologiques Préventives, Centre-Île de France, 93120 La Courneuve, France
[b] Institut Français d'Etudes Andines, IFEA, UMIFRE 17 CNRS/MAEDI, La Paz, Bolivia
[c] Univ. Grenoble Alpes, Univ. Savoie Mont Blanc, CNRS, IRD, Univ. Gustave Eiffel, ISTerre, 38000 Grenoble, France
[d] Centre de Recherches en Archéologie et Patrimoine, Université libre de Bruxelles, 1050 Bruxelles, Belgium
[e] UMR 7619 METIS, Sorbonne Université, CNRS, EPHE, 75005, Paris, France
[f] Instituto de Investigaciones Antropológicas y Arqueológicas, Universidad Mayor de San Andrés, La Paz, Bolivia
[g] Laboratorio de Hidroquímica, Instituto de Investigaciones Químicas, Universidad Mayor de San Andres, Campus Universitario de Cota Cota, Casilla 3161, La Paz, Bolivia

ARTICLE INFO

Handling Editor: Dr Mira Matthews

Keywords:
Tiwanaku culture
Canals surface morphology
Geophysical survey
Palaeoenvironments
Geoarchaeology
Late holocene
Andes

ABSTRACT

Water management enabled the development of ancient societies allowing them to ensure agropastoral production and manufacturing activities. In the Andes, near the shore of Lake Titicaca, the city of Tiwanaku (Bolivia) is one of the largest pre-Hispanic urban centres in South America. Abrupt climate changes in the high-altitude Altiplano during the late Holocene likely forced the population to develop water management strategies. So far, knowledge concerning the existence of a water network around the city of Tiwanaku is limited to hypotheses derived from surface and aerial observations. In this study, geoscience techniques (morphology, geophysics, sedimentology and chronostratigraphy) helped to reconstruct the canals' morphology and their flow dynamics, along with their chronology of operation in a context of hydroclimatic change. Two ca. 30 m large canals bypassing the monumental core and supplied by a shallow water table and multiple tributaries, connected the agricultural and the urban areas. The structure and organization of the network testify to an elaborate knowledge of the local hydrology by the former builders of the city. It ensured water supply and flood management in relation to the extreme intra- and inter-annual variability of precipitations in the central Andes. The palaeogeographical and landscape reconstruction demonstrates that canals were set from natural features during the early Late Formative period (200 BCE to 200 CE) during a wet period likely for water resource management needs. During the Tiwanaku state (before 800 CE), the filling of the canal network with soil and sediment suggests a major change in its use, and possibly its partial abandonment, during a major restructuration of the site, in a period of increased regional precipitation.

1. Introduction

Water management was crucial for the development of ancient societies, primarily to ensure agropastural production but also for essential needs (drinking, food processing, cooking, bathing, and various manufacturing), and sociopolitical purposes. Around the world, ancient societies developed advanced hydraulic systems to face water scarcity or control water collection, transport and sustainability (Yevjevich, 1992). Numerous archaeological studies have provided evidence of the development of such systems as long ago as 3000 years BCE in Mesopotamia (Wilkinson et al., 2014), during the first millennium BCE in Ancient Greece (Angelakis and Spyridakis, 2010), the North China Plain (Storozum et al., 2018), South Asia and in the New world (Ortloff, 2009). The development of irrigation networks was of political importance (Wittfogel, 2017) as it enabled agricultural societies to intensify agricultural production. However, such networks required specific maintenance and

* Corresponding author. Institut National de Recherches Archéologiques Préventives, Centre-Île de France, 93120 La Courneuve, France.
E-mail address: marc-antoine.vella@inrap.fr (M.-A. Vella).

https://doi.org/10.1016/j.quascirev.2023.108475
Received 3 September 2023; Received in revised form 14 December 2023; Accepted 15 December 2023

developments depending on hydroclimatic or social constraints (Purdue, 2015).

In the Americas, one of the best examples of a human-built landscape is the Lake Titicaca Basin (Bolivia/Peru; Fig. 1a) which has long been a major centre of agricultural production and the home of several important pre-Hispanic societies (Erickson, 2000; Delaere et al., 2023). Amongst them, Tiwanaku is one of the largest pre-Inca cultures, and it dominated the southern half of the central Andes between the 5th and 11th centuries CE (Kolata, 2003). The rise of this society began on the shores of Lake Titicaca at an elevation of 3810 m above sea level (asl; Fig. 1b). It occurred thanks to the development, amongst others, of agro-pastoralism, commercial and religious networks, and the management of water resources (Browman, 1981; Kolata and Ortloff, 1989; Bandy, 2005). Although the lake provided a great water reservoir, extreme variability in regional precipitation on the Altiplano (Baker et al., 2001) forced this early society to develop water management strategies for urban and agricultural water supply.

In the pre-Hispanic urban centre of Tiwanaku, presently a UNESCO World Heritage site, the presence of an ancient hydraulic network has been proposed by archaeologists (Posnansky, 1945; Kolata, 2003; Lasaponara and Masini, 2014; Ortloff and Janusek, 2016; Pérez González and Gallego Revilla, 2020). Based on terrestrial, aerial, and

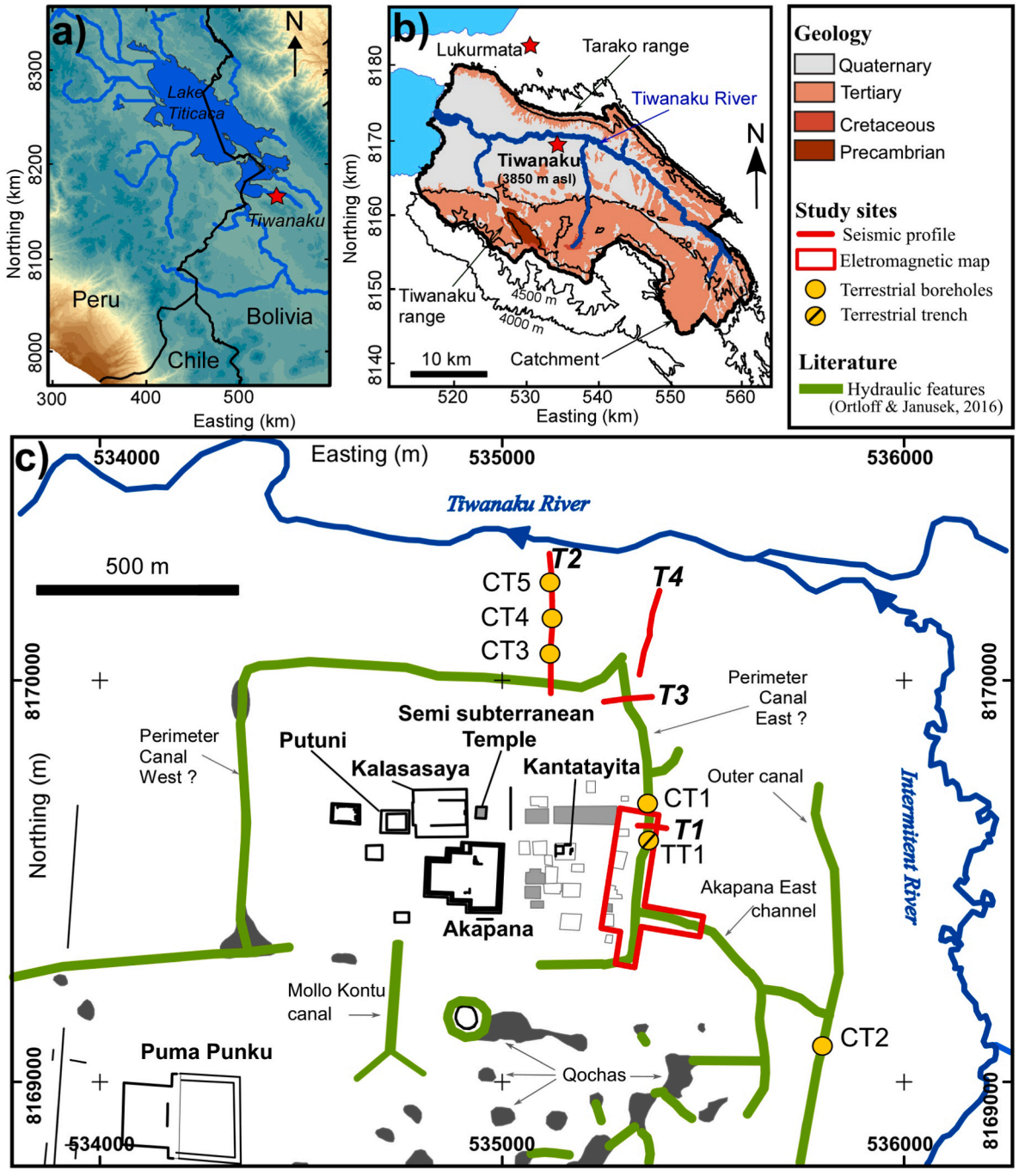

Fig. 1. Presentation of the study site. a) Location of Tiwanaku in the Lake Titicaca Basin. b) Simplified geological map derived from GEOBOL (1995). c) Location of geophysical measurements (electromagnetic mapping, seismic profiling), boreholes and trench. The main archaeological monuments of the city of Tiwanaku with the location of the hydraulic features described in the synthesis of Ortloff and Janusek (2016) are also presented. Coordinates are metric and expressed in the UTM 19 S system with the WGS84 geodetic model.

satellite observations, these studies have suggested the presence of a large quadrangular moat-like structure encircling the ceremonial centre of the city and connected to at least three canals supplied by local rivers and wetlands (Fig. 1c). Described as a part of an artificial landscape, the canals are thought to have played a key role in Tiwanaku's sophisticate agricultural techniques for the retention of water and the management of seasonal floods, or as a structure of symbolic and ritual importance, separating the elite residences from the surrounding urban peripheries (Posnansky, 1945; Kolata, 1993). To date, excavations and geophysical prospecting have revealed the presence of subterranean canals, made of crafted sandstone and andesite, within the monumental core (Kolata, 1993; Couture and Sampeck, 2003; Janusek and Kolata, 2004; Janusek and Bowen, 2018; Vella et al., 2019). However, no investigation around the core has validated the existence of the canals nor documented their morphology, connection to groundwater and chronology of operation.

In order to bring new insights into the water management of the city of Tiwanaku, we combined watershed morphology analysis, subsurface lithology mapping and imaging, lithology analysis and archaeological analysis. Finally, six new radiocarbon ages allowed us to refine the chronological framework of the canals. Given the current knowledge on the evolution of the landscape of the city of Tiwanaku, this paper aims i) to confirm, at some key locations, if there is awater network around Tiwanaku city and, if so, to define its morphology and its relation with the surface and groundwater network; ii) to propose a chronology of use for the canal network in relationship with the occupation of the city and the palaeoenvironmental context.

2. Geomorphological and archaeological setting

The pre-Hispanic city of Tiwanaku (535 000 E; 8 169 500 N) is located on the Bolivian Altiplano at 3850 m asl near the left bank of the middle Tiwanaku River (TR) Valley (Fig. 1a and b). The geological basement is made of Precambrian to Tertiary sedimentary rocks which outcrop in the Taraco and Tiwanaku ranges, to the north and south of the valley, respectively (Fig. 1b). Between these two roughly NW-SE-oriented ranges, the depression corresponding to the TR valley is filled up with Quaternary sediments (GEOBOL, 1995; Vella and Loget, 2021). These sediments show alternations of lacustrine and fluvial layers which reflect Lake Titicaca level variations (Weide et al., 2017), originating from glacial-interglacial cycles, themselves caused by Quaternary climatic oscillations.

These quaternary sediments are mantled by late Holocene-aged soil profiles. They were incised by the TR which follows a meandering course to the southern Lake Titicaca sub-basin (3809 m asl), namely "Lago Menor" or "Wiñaymarka". The lake is 9 m-deep on average (Dejoux and Iltis, 1992) and its level has varied up to 15 m during the late Holocene (Abbott et al., 1997; Mourguiart et al., 1998; Fritz et al., 2006; Weide et al., 2017; Guédron et al., 2023). On a large scale, the region exhibits a morphology of a badlands environment, particularly affecting the Taraco range (not shown here but visible on freely available global Digital Elevation Models). On a smaller scale, smooth relief prevents the observation of gullying features.

Tiwanaku (Fig. 1c) includes an urban core of 40–65 $\times$ 10^3 m^2 composed of a monumental complex and urban residential compounds surrounded by agro-pastoral areas (Ponce Sanginés, 1972; Janusek, 2003a; Ortloff and Janusek, 2016). Archaeological studies date the first monumental buildings (the semi-subterranean Temple and the Kalasasaya Platform) to the Late Formative Period, around 100 BCE to 400 CE (Kolata, 2003; Stanish, 2003; Vranich and Stanish, 2013). Between ca. 600 CE to 1000 CE a major extension of the urban core accured with the construction of new monuments (Putuni, the Akapana Pyramid, and probably the Kantatayita Temple) (Janusek, 2004; Vranich and Stanish, 2013). At that time the urbanized area reached ca. 6 km^2, hosting between around 15 to 20 thousand inhabitants (Kolata, 2003; Stanish, 2003).

3. Materials and methods

To answer the scientific questions, a multidisciplinary geoscientific approach was adopted. The study first combined high-resolution topography from a recent High-Resolution Digital Surface Model (HR-DSM) and geophysical prospecting (electromagnetic induction mapping and seismic refraction imaging), along with sediment chronostratigraphy, to quantitatively document the morphology and the spatial distribution of this hydraulic network. The dated canal sedimentary profiles were then compared to published reconstructions of regional paleohydrology to position the chronology of the operation of the canal network in a palaeoenvironmental context.

3.1. Surface morphology mapping

The quantitative analysis of surface morphology in locations with gentle slopes and smooth relief requires high resolution data to potentially connect topographic depressions and evaluate the flowing directions of surface water. The recently published UNESCO HR-DSM (Gallego-Revilla and Pérez-González, 2018; Pérez González and Gallego Revilla, 2020) was determined from optical images acquired with a drone equipped with a high-resolution camera (4896 $\times$ 3672 px^2). The dataset covers a surface of 4.1 km^2 and consists of 911 overlapping images with an average ground sampling distance of 3.8 cm. Images were processed with the pix4Dmapper software (Pix4D SA, 2016). They were orthorectified and georeferenced using 5 Ground Control Points (GCP) acquired with a total station and which provided an average root mean square error of 2 mm. The generated point cloud presents an average density of 51 points per m^2. This point cloud was then interpolated to produce a continuous DSM with a planimetric resolution of 0.16 m. From this HR-DSM, a watershed analysis was conducted using the D8 algorithm (Tarboton, 1997). The algorithm provides a distribution of connected depressions and allows the reconstruction of potential watersheds. The presence of modern structures (such as roads, railways, ditches, etc.) might bias the analysis and generate watersheds. To remove this from the interpretation, filtering operations mainly consisted in deleting these recent anthropogenic structures. They were identified using present-day printed maps (*e.g.* geological, topographic and street maps) and aerial photographs. Anthropogenic modern features were identified by observation of linear structures generally not oriented along the main slope. In contrast, natural structures are more sinuous and also oriented preferentially along the slope.

3.2. Subsurface lithology mapping and imaging

Two geophysical methods were used to indirectly retrieve the distribution of lithological and hydrological parameters of the subsurface: electromagnetic induction (EMI) mapping and seismic refraction (SR) imaging. These 2two methods are widely used and described in reference books (Telford et al., 1990) and will be briefly exposed hereafter.

The EMI survey (location in Fig. 1c) was performed using a CMD Explorer (GF Instruments, Brno, Czech Republic). The device has three receiver (Rx) coils at different offsets from the transmitter (Tx) coil and thus provides values of apparent electrical conductivity (σ_a, generally expressed in $mS.m^{-1}$) integrated from the surface down to various depths (around 2.2, 4.2 and 6.7 m with horizontal coplanar coils). The measured parameter σ_a is a type of volume-averaged apparent electrical conductivity of the soil. The method allows sub-surface structures to be mapped rapidly and without contact. It consists of the transmission of an oscillating primary magnetic field from a transmitter coil above the ground. Electrical currents are induced in the ground conductive structures and generate a secondary magnetic field as a response. A receiver coil then measures both fields. The quadrature component of the ratio between both fields is directly related to the apparent electrical conductivity of the soil when the offset between transmission and reception is much smaller than the depth of penetration of the

transmitted signal in the ground. Measurements in the field were conducted in the horizontal coplanar (HCP) mode and results with two coil separations corresponding to penetration depths of around 2.2 and 6.7 m will be presented. Data were processed with the WuMapPy package (Marty et al., 2015). Results are presented as maps showing the spatial distribution of σ_a. Variations in apparent conductivity can be related to changes in mineralogical content, water saturation and ionic charge, porosity, etc. Without external information, it remains difficult to relate the measured parameter to a physical parameter, and the interpretations will mainly be conducted in terms of geometrical description.

Seven seismic refraction profiles were conducted using a Geode seismograph (Geometrics, San Jose, USA) to image the superficial alluvial deposits and geological formations surrounding the Tiwanaku site. Each profile was obtained with 24 horizontal and vertical geophones linearly spread with a constant separation of 3–5 m, to measure compressional (P) and shear (S) wave velocity, respectively. Both parameters are related to the subsurface stiffness. However, in the presence of a water table, P-wave velocity dramatically increases. This geophysical parameter is then suited to detect saturation. On the contrary, shear waves do not exhibit rapid velocity change towards saturation. They furthermore provide a much better resolution. The seven profiles were gathered in four, 2D profiles, labelled T1 to T4 (location in Fig. 1c). Profiles T1 and T3 were located across a previously mapped canal, east of the monumental complex, to determine its geometry. Profiles T2 and T4 were located in the fluvial plain, north of the monumental complex, to investigate its stratigraphy and hydrological setting. First arrival times were manually picked and further inverted with the pyGIMLi package (Rücker et al., 2017) to provide 2D images of the distribution of seismic velocity. All inversions provided satisfactory numerical results with χ^2 values around 1 and relative root mean square errors ranging between 4.2 and 11.6 % (see Supplementary Information S-1 for details on the statistics of inversion and results).

3.3. Lithology analysis

Five auger boreholes (CT1 to CT5; location in Fig. 1c) were collected in the perimeter and outer canals (CT1 and CT2; 3 and 1.5 m deep, respectively), and in the alluvial plain of the Tiwanaku River (CT3, CT4 and CT5; 1, 2 and 1 m deep, respectively). The strategy of boreholes collection was based on results obtained from geophysical surveys to document the chronology and sedimentary dynamics between the channels and the alluvial plain. Boreholes were sampled using a 250 mm-width auger. At each site, the boreholes were duplicated with a vertical offset of 0.1 m to recover the entire stratigraphy. Borehole collection was impossible within layers located below the water table and composed mainly of non-cohesive sandy deposits. Sample colour description was performed using the Munsell chart. Samples were then subdivided into 5 to 10-cm-long sections, collected in plastic bags and homogenized within the bags. Samples were then dried at 105 °C, sieved at 2 mm and the collected fraction <2 mm was kept for grain size distribution and Organic Matter (OM) analysis. The grain-size distribution of particles smaller than 2 mm was measured using laser diffraction with an LS 13 320 particle size analyser (Beckman Coulter). Samples were prepared following the protocol proposed by Di Stefano et al. (2011) and analysed in triplicates to ensure repeatability. OM content was determined through Loss On Ignition at 550 °C ($LOI_{550°C}$) (Heiri et al., 2001).

3.4. Chronological analysis

Radiocarbon dating was conducted on six samples (charcoal and bones) collected in the boreholes and in a terrestrial trench (see below). Analysis of terrestrial samples was conducted at the Poznan laboratory (Poland). Radiocarbon ages were calibrated to calendar years Before Present (cal. yr BP) using the calibration curve for the Southern Hemisphere SHCal20 (Hogg et al., 2020) and post-bombs (Hua et al., 2013).

3.5. Archaeological analysis

Archaeological prospecting was performed in a trench (TT1 in Fig. 1c) located on the edge of the perimeter canal in the eastern part of the monumental core. In each stratigraphic Unit (SU), archaeological artefacts were recovered, classified and numbered for a defined volume of collected sediment before their ceramological characterization. From the total number of artefacts (x) per archaeological stratigraphic layer (SU), the Anthropogenic Activity Rate (AAR) (Delaere, 2017) was assessed using a frequency index (x/SU). Frequency variability and the identification of frequency peaks allow the identification of the most important events of anthropogenic activities according to the abundance of archaeological material.

4. Results

4.1. Identification of surface hydrological features with high-resolution topography

Both the general slope and high-resolution topographic cross-sections obtained from the high-resolution Digital Surface Model (HR-DSM) were used to distinguish between natural and anthropogenic features and to further select coring and geophysical prospecting sites. The HR-DSM is presented in Fig. 2a. The mapped area from the South to the northern limit of the monumental area has a gentle slope (around 3%) to the North. In the central area, almost all identified positive topographical anomalies were tied to the archaeological structures of the monumental complex. These structures, which were identified by previous archaeological studies, are the Mollo Kontu mound (MK), the Pumapunku (PP) and the Akapana Pyramids (AP) (Fig. 2b) (Couture and Sampeck, 2003; Janusek, 2004). The monumental core is bounded to the West and the North by the topographically lower modern terraces, where numerous identified depressions allowed the distinction between natural water streams and anthropogenic features. The watershed analysis is presented in Fig. 2b, and filtered from the most probable modern structures, identified from topographic maps and aerial photographs. For example, the old Guaqui-La Paz railway line, which runs west-east to the south of the Akapana pyramid, was excluded from the analysis to provide pre-Hispanic topographic features. In addition, although the pre-Hispanic raised fields are no longer visible today, the general topography (depressions, elevations, water table, etc.) is likely unchanged and should allow the understanding of the global hydraulic system.

Identified natural streams consist of i) two perennial streams encircling the core and flowing northward, i.e., the Challa Jahuira River (CJR) in the West, and the Tiwanaku River (TR) in the North, and ii) an intermittent river to the East (labelled Eastern Intermittent Stream, EIS) which joins the TR to the north (Fig. 2a). Amongst anthropogenic depressions, two types of hydrological features were identified: i) linear topographical anomalies corresponding to probable historical canals, and ii) the agricultural fields, lagunas or ponds (Fig. 2b). First, two linear, U-shape features surrounding the West (from markers A to B in Fig. 2b) and East (C to D to E in Fig. 2b) sides of the monumental core correspond to the perimeter canal reported by archaeologists (Posnansky, 1945; Kolata, 2003; Ortloff and Janusek, 2016). These two features are oriented North (cross-sections A-B and C-D-E in Fig. 2c) and join the low-level terrace in the TR alluvial plain which then flows North-West to the TR. This U-shape feature is connected to two different types of possible secondary canals or an intermittent river; i) a linear topographical anomaly in the South-West side oriented westward (A to H in Fig. 2b); ii) the Mollo Kontu Canal (MKC, K to I in Fig. 2b) in the South oriented Northward (in Fig. 1c); and iii) a linear depression in the South-East (G to F in Fig. 2b) located on the plateau with a broadly north-west-dipping slope (section F-G in Fig. 2d) and known as the Akapana East Channel (Fig. 1c).

Second, in the lowermost depression located North, agricultural

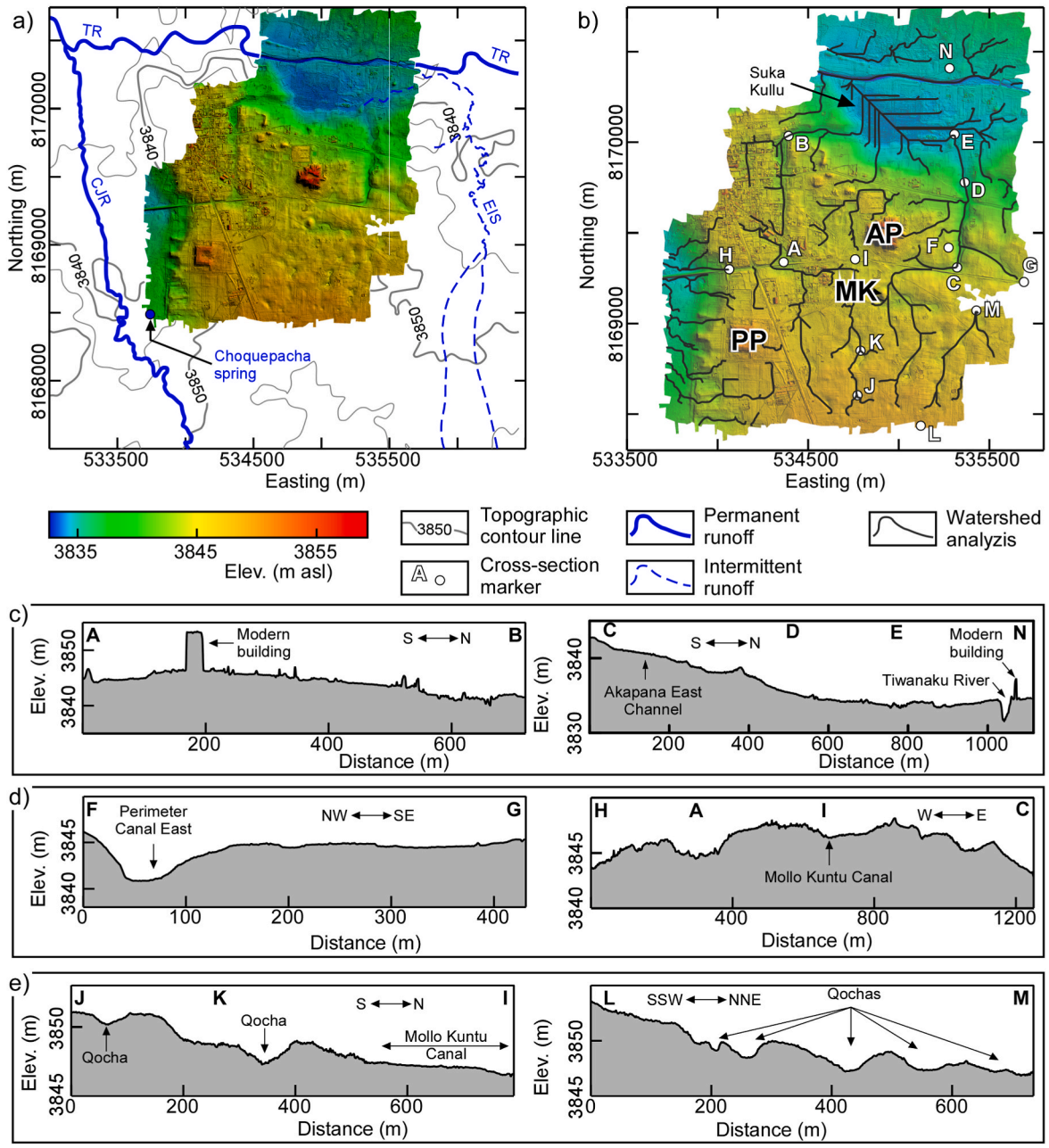

Fig. 2. High-resolution topographic analysis of the study site. a) High-resolution Digital Surface Model (Gallego-Revilla and Pérez-González, 2018; Pérez González and Gallego Revilla, 2020). b) Watershed analysis. TR: Tiwanaku River; CJR: Challa Jahuira River; EIS: Eastern Intermittent Stream; AP: Akapana Pyramid; PP: Pumapunku; MK: Mollo Kontu mound. Letters A to N: topographic cross-section markers; c) Topographic cross-sections A-B and C-D-E across the perimeter canal. d) Topographic cross-sections F-G and H-A-I-C across secondary canals. e) Topographic cross-sections J-K-L-I and L-M across anthropogenic features (qochas).

raised fields, namely "suka kullu", are found (Fig. 2b). This depression is a modern agricultural planting area constituted by an elevated soil band of around 2–10 m wide and up to 200 m long, which explains the perpendicular geometry of the watershed analysis. It was reconstructed by local Aymara communities in an experimental field rehabilitation program performed in the 1980s (Erickson, 1992; Kolata and Ortloff, 1996). In the South, lagunas or ponds were identified, along with numerous sunken basins named "qochas" (Fig. 2e). They are found dendritically linked to each other and seem connected to both the MKC (from J to K to I in Fig. 2b and e), and another canal oriented North (from L to M in Fig. 2b and e) and most probably joining the Akapana East Channel to the North after Ortloff and Janusek (2016) (Fig. 1c).

4.2. Geophysical characterization of canal morphology

The electromagnetic induction (EMI) maps in Fig. 3 present the spatial distribution of the apparent electrical conductivity (σ_a). Their location is shown in Fig. 1c. They were performed in the South-East area of the monumental centre with depths of investigation of ~ 2.2 m (Fig. 3a) and ~ 6.7 m (Fig. 3b). For the shallowest investigation, it shows the presence of a North-South-elongated conductive zone (>45 mS m^{-1}, labelled a in Fig. 3a), matching the path of the previously identified perimeter canal. Laterally to this elongated, conductive zone, σ_a is lower (<40 mS m^{-1}; labelled b in Fig. 3a). The evidence of residential occupation was found in archaeological excavations (AKE-1, AKE-2 and AKE-1M in Fig. 3a; details in Supplementary Information S-4) (Janusek,

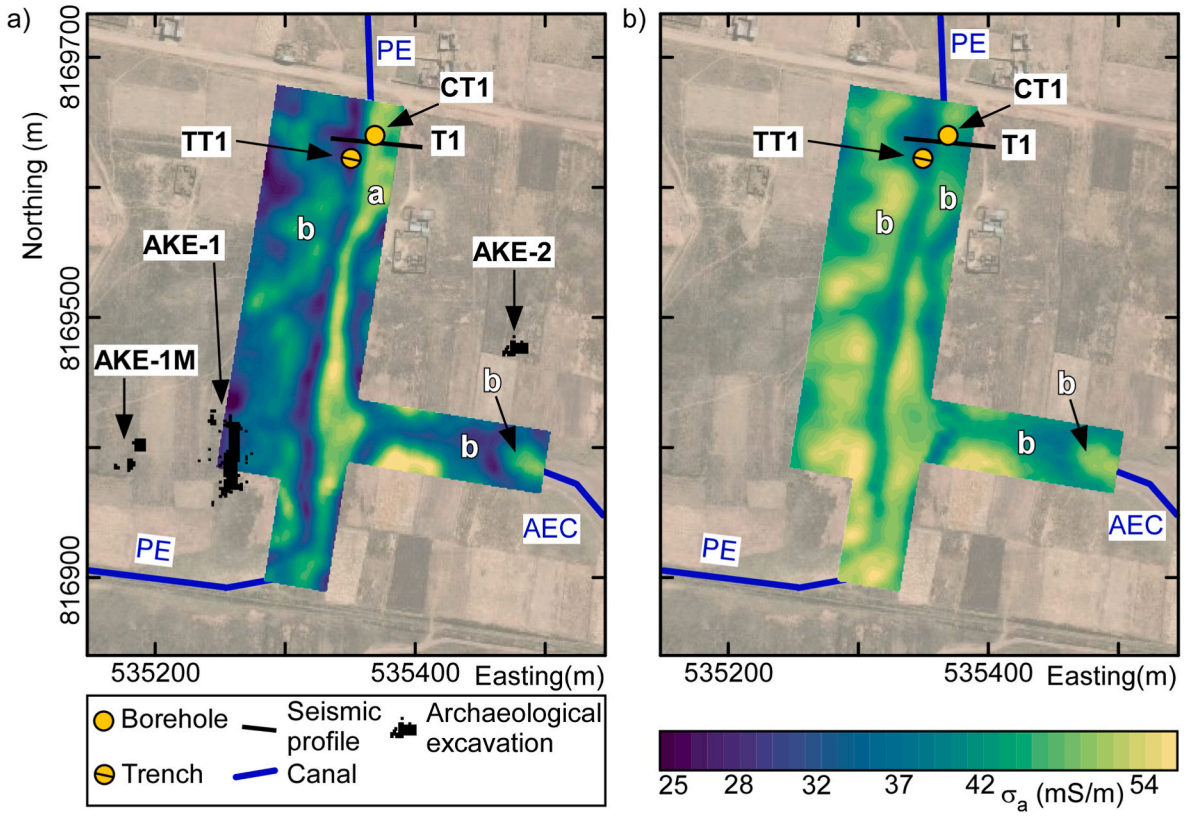

Fig. 3. Electromagnetic induction map of the eastern part of the perimeter canal (location in Fig. 1c) for depths of investigation of around a) 2.2 m and b) 6.7 m. The location of PE and AEC is deduced from Fig. 2. References to archaeological excavations AKE-1: Janusek (1994); Janusek (2003a); Janusek (2004); and to AKE-1M and AKE-2: Janusek (1994); Janusek (2003b); Janusek (2004). Labels a and b correspond to geophysical units that are described in the text.

2003b). This unit b exhibiting low σ_a then probably attests to different subsurface properties (mineralogy, porosity, water content, etc.) than unit a. The western termination of the AEC was also mapped. Unlike the PE, no conductive layer is observed in the topographic depression, except at the eastern limit of the map (label b with the black arrow in Fig. 3b). On the contrary, it shows low σ_a values (<40 mS m^{-1}) comparable to unit b. Without further external observation, this zone remains difficult to interpret. However, from the absence of a conductive

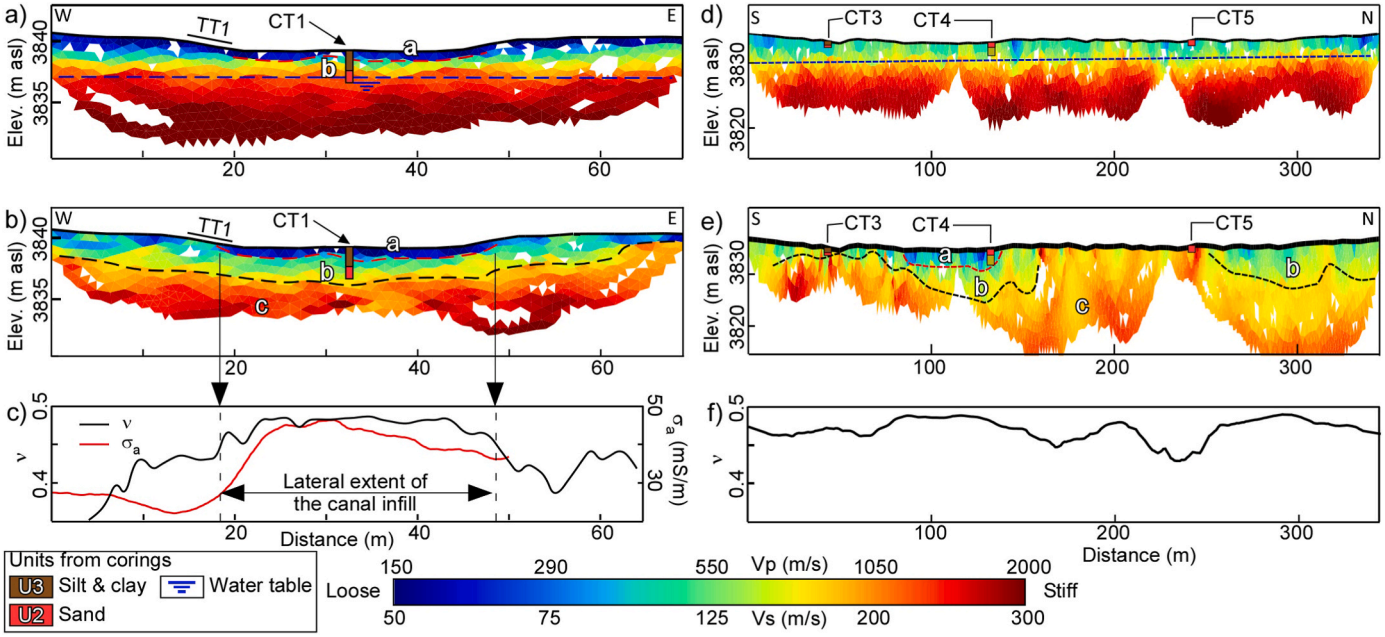

Fig. 4. Seismic refraction results of profiles T1 (a, b and c) and T2 (d, e and f). Profiles are located in Fig. 1c. From top to bottom: P-wave velocity Vp (a, d), S-wave velocity Vs (b,e) and Poisson's ratio ν (c,f). Corings are indicated. An apparent electrical conductivity cross-section along profile T1, and extracted from Fig. 3, is also represented in Fig. 4c. Note that the vertical and horizontal scales are not similar between the 2 profiles.

and elongated feature along the axis of the topographic depression, it could be hypothesized that canal deposits, if they exist, have a limited spatial extent in both width and depth. The deeper investigation of the EMI map (down to ca. 6.7 m; Fig. 3b) exhibits more homogeneous conductivity in the range 35–50 mS m^{-1} over the whole investigated surface. In the context of the study site, it is mainly interpreted as saturated conditions below ~ 3 m depth (see seismic results below) with water potentially enriched in dissolved gypsum originating from the Tertiary Kollu formation (Tkk) (GEOBOL, 1995).

Seismic images are presented in Fig. 4 and the identified units are labelled similarly to the EMI map when possible. Profiles T1 and T2 were conducted across the PC (Fig. 1c) and exhibit slow P-wave velocity values (*Vp*) over the first 2 m (Vp < 300 m s^{-1}; Fig. 4a and d). Then, *Vp* strongly increases up to more than 1500 m s^{-1} below around 2 m depth.

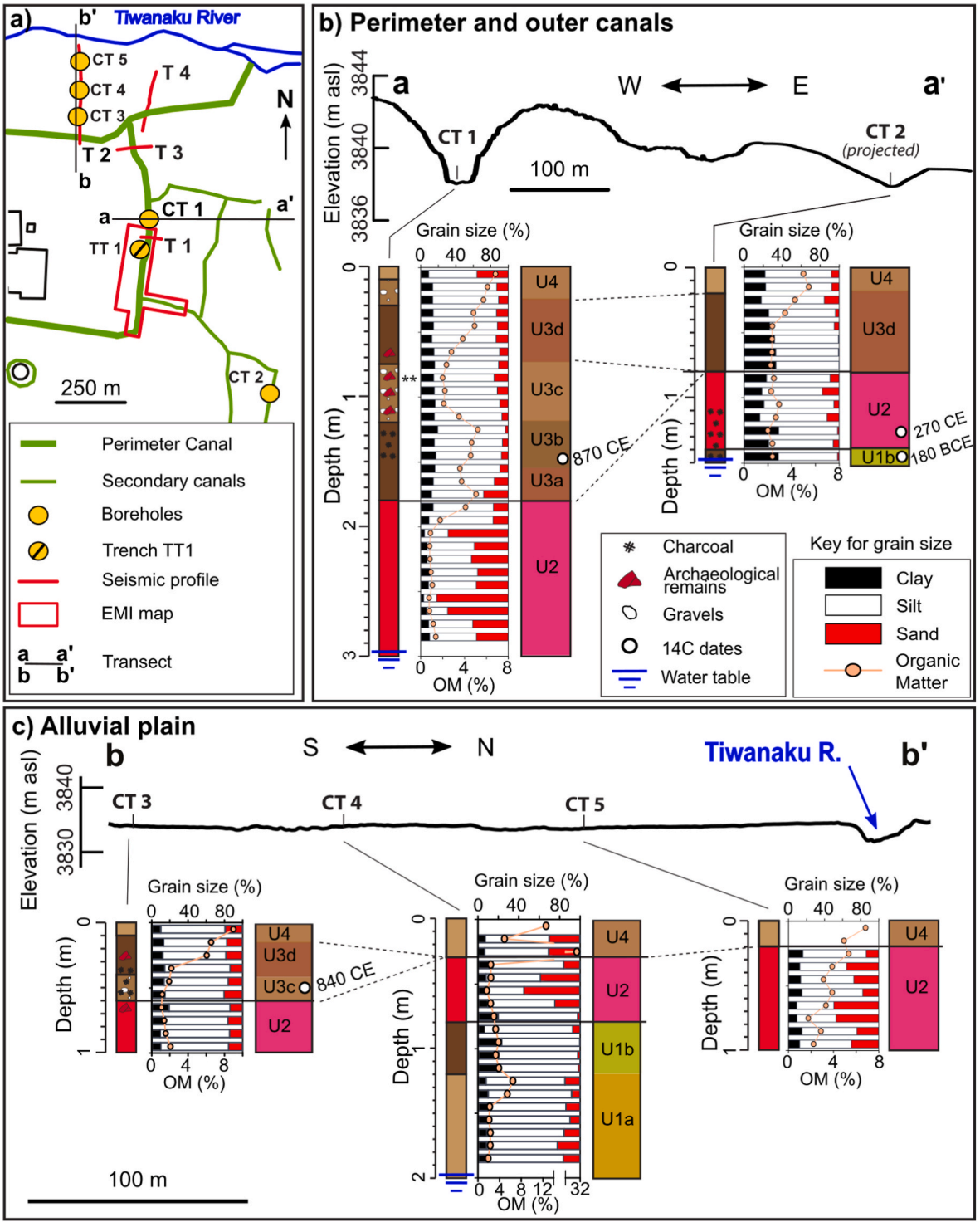

Fig. 5. Analysis of boreholes CT1 to CT5. a) Location of the boreholes. b) Boreholes CT1 and CT2 along transect aa' in the perimeter and outer canals. Boreholes were conducted in July during the dry season, illustrating the lowermost level of the water table, which was reached in both boreholes. U1 to U4: stratigraphic units (see text for details). c) Boreholes CT3, CT4 and CT5 along transect bb' in the alluvial plain (same legend as for Fig. 5b). The water table was reached at the base of CT4. 10 over 13 artefacts were recovered from units 3c and 3 d in CT1 and dated from the post-Tiwanaku epoch.

On profile T1, this interface (blue dashed line in Fig. 4a and d) is horizontal and coincides with the presence of the water table identified in borehole CT1 at this depth (see description further). By analogy, it also corresponds to the water table in profile T2. However, although it is difficult to observe from the figure because of the vertical scale, this interface slightly dips towards the South with a difference in elevation of 2 m along this 345 m-long profile, corresponding to a slope of around 0.6%. The S-wave velocity (*Vs*; Fig. 4b and e) image offers a better resolution and allows the distinguishing a low-velocity layer ($Vs < 75$ m s^{-1}) with a maximum thickness of 2 m located between 20 and 50 m along profile T1 (unit a in Fig. 4b). This layer is not detected along profile T2 (Fig. 4e). Unit b is observed at the surface before 20 m and after 50 m along T1 (and all along T2), with *Vs* in the range 100–150 m s^{-1}. It is around 3 m-thick and locally up to 10 m thick in T2 (between abscissa 40 and 50 m). Below, *Vs* is higher than 200 m s^{-1} and up to more than 300 m s^{-1} (unit c) and could indicate the Qcf formation. Finally, the Poisson's ratio (ν) of the first, unsaturated, 2 m below the surface was computed from P and S-wave velocity along the profiles (Fig. 4c and f for T1 and T2, respectively). The apparent electrical conductivity extracted from the EMI map (Fig. 3a) was added to T1. For T1 (Fig. 4c), both parameters covary and reach their highest values ($\nu > 0.45$ and $\sigma_a > 40$ mS m^{-1}) between 20 and 50 m along the profile, indicative of undrained, fine-grained sediments with a significant water content (Telford et al., 1990; Sharma, 1997). The lateral limits of this zone also correspond to those of the topographic depression along the profile (Fig. 4b), in agreement with the presence of an ancient channel at this location. The Poisson's ratio does not vary much along T2 (Fig. 4f) and presents values around 0.45. Similar analysis were conducted on profiles T3 and T4, the results of which are detailed in Supplementary Information S-2. Briefly, and notably for P-wave velocity, similar velocities were observed with depths to the interface located at around 2 m. The slight difference in elevation (around 0.7 m) along the 215 m-long profile T4 suggest a dipping of the interface towards the South with a slope of around 0.3 %.

4.3. Canal lithostratigraphy and chronology

Fig. 5 presents the lithological description of boreholes CT1 to CT5 collected at the study site (location in Fig. 5a). The boreholes were collected in both the perimeter and outer canals (Fig. 5b) and the alluvial plain (Fig. 5c). The water table was reached in CT1, CT2 and CT4 at respective depths of 3, 1.5 and 2 m (respective elevations of the water table of 3835, 3848.5 and 3831 m asl). All boreholes depict a consistent stratigraphy with four main units, U1 to U4, of variable thickness.

The first basal unit (U1) was collected in CT2 (Fig. 5b) and CT4 (Fig. 5c). It is yellowish-red (5YR4/6 to 5YR5/6), with a grain size distribution dominated by silts and clays with average contents of 62–76 % and 20–36 %, respectively, and with no gravel. It also shows an OM content lower than 2.5 % on average. Unit U2 was observed in all boreholes. It is red (10R4/8) and dominantly composed of silt and sand-size particles (*e.g.* average sand is 45 % in CT1). It is the most OM-depleted layer with content ranging from 0.8 to 3.8 %. This layer is an analogue of the modern red TR bed sediment and likely indicates a turbulent hydrodynamic regime, typical of channelized sedimentation where fine-grained sediments are entrained from alluvial stream beds (Sutherland, 1967). In contrast to CT1, the unit U2 of the outer canal borehole (CT2 in Fig. 5b) is dominated by silts, which suggests a less turbulent hydrodynamic regime in comparison with the perimeter canal. The overlaying unit U3 displays a transition from red (2.5YR4/6) to yellowish-red (5YR5/6) layer, dominated by silty-clay particles enriched in OM (up to 6 %) with several layers enriched in gravels (*e.g.* up to 10 % in sub-unit 3c). This granulometric pattern supports a return to less turbulent deposition as those of the upper part of Unit 1. This unit is extensively developed in the perimeter canal (CT1) with four subunits composed of variable OM concentrations but a constant granulometry dominated by silts. In particular, the two lowermost subunits 3a and 3 b, which contain numerous charcoals and ceramic debris, are only found in this core. On the other hand, the two upper subunits are only encountered in the perimeter canal (CT2) and the most southern part of the alluvial plain transect (CT3). Finally, the uppermost unit U4 corresponds to the modern reddish yellow (5YR6/6) till layer with a silty-sand texture and the highest OM content observed in boreholes (up to 32 % in CT4). This layer is found in the entire set of collected boreholes.

The first stratigraphical units U1 and U2 were bracketed chronologically by 6 radiocarbon ages performed on macro-remains (two ages among the eight were modern and consequently rejected; Fig. 5 and Supplementary Table S2) collected in the different profiles. The bottom unit (Unit 1, CT2 and CT4) is dated before ca. 180 BCE and ends before 270 CE. Only one organic remnant was found in Unit 2, hence the age of this red sediment layer is estimated between after ca. 180 BCE and before ca. 800 CE, the youngest age obtained in Unit 3.

4.4. archaeological excavation

Trench TT1 was excavated at the edge of the perimeter canal to document the archaeological context, and the results are presented in Fig. 6. The archaeological context offers supplementary insights into both chronology and the utilization of the canal. This, in turn, grounds the discussion within the socio-cultural context that characterizes the studied archaeological site. Two additional radiocarbon ages (680 CE and 820 CE) bracket the Stratigraphic Units (SU) 13 and 10, located above the canal sediment deposits (*i.e.* Unit 3 in boreholes CT1 and 2). They support a change in sedimentation after ca. 680 CE that was observed in the boreholes.

Within the trench, 2525 ceramic fragments were retrieved from this excavation, identified and contextualized with the same lithostratigraphy as the boreholes when possible (details are given in Supplementary Information S-3). The size and state of preservation of the ceramic fragments, often less than 1 cm^2, do not allow a reliable chronological assessment. Overall, Tiwanaku sherds are found in all stratigraphic units, but with a greater abundance from SU 5 to 11. However, of the 2525 fragments, the shapes of 408 fragments could be determined (16.16% of the total). These mainly represent *jarras/vasijas* (62.34%), *keru/tazon* (19.01%), *ollas* (12.71%) and *tinajas* (3.76%), i.e. vessels associated with the use of water, whether for cooking, storing or consumption of fermented beverages. The ceramological study supports previous archaeological excavations (Janusek, 1994, 2004). When considering the entire set of artefacts, the calculation of the anthropogenic activity rate (AAR, number of artefacts per stratigraphic unit; Fig. 6) gives complementary information on the chronology and phases of human activity associated with the canal. No ceramic fragments were found in the canal (SU 15 & 14). A Qeya (LF2) decorated sherd was found in SU13. SU12, which is contemporary to the reddish sediments found in the perimeter canal (*i.e.* Unit 2 in CT1), has the highest AAR, attesting to the filling of the canal or a major occupation of the side of the canal between 680 and 820 CE (Fig. 6). In SU11, AAR sharply declines but is followed by an increase in SU 10 to 5 to reach a second maximum in the SU5 which corresponds to the last level where the Tiwanaku period artefacts remain abundant (800–1110 CE). SU4 to SU1 are the only units where the form allows for chronological discrimination, with forms globally posterior to the Tiwanaku period.

5. Discussion

5.1. comprehensive overview of the channel network (geomorphology and hydrological functioning)

The combination of geoscience and archaeological evidence confirms the presence of a sophisticated hydraulic network around the monumental centre of the city of Tiwanaku and provides the dimensions, flow directions, and most probable water inlets into the canals. The major identified canals and their most probable flow directions

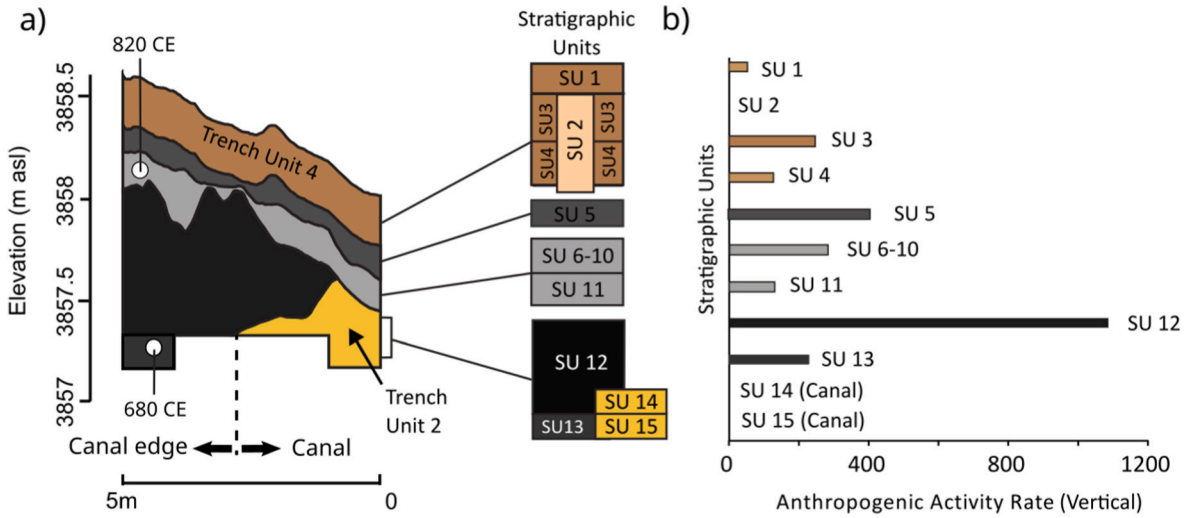

Fig. 6. Archaeological trench TT1 (location in Fig. 1c). a) Geometry and stratigraphy of the trench (left) along with the determined stratigraphic units SU (right). Note that Trench Units 2 and 4 are equivalent to those of coring CT1 in Fig. 5a b) Vertical Anthropic Vertical Contextualization (AVC) in each stratigraphic unit. AAR is expressed as the number of artefacts per stratigraphic unit. Details are provided in Supplementary Information S-4.

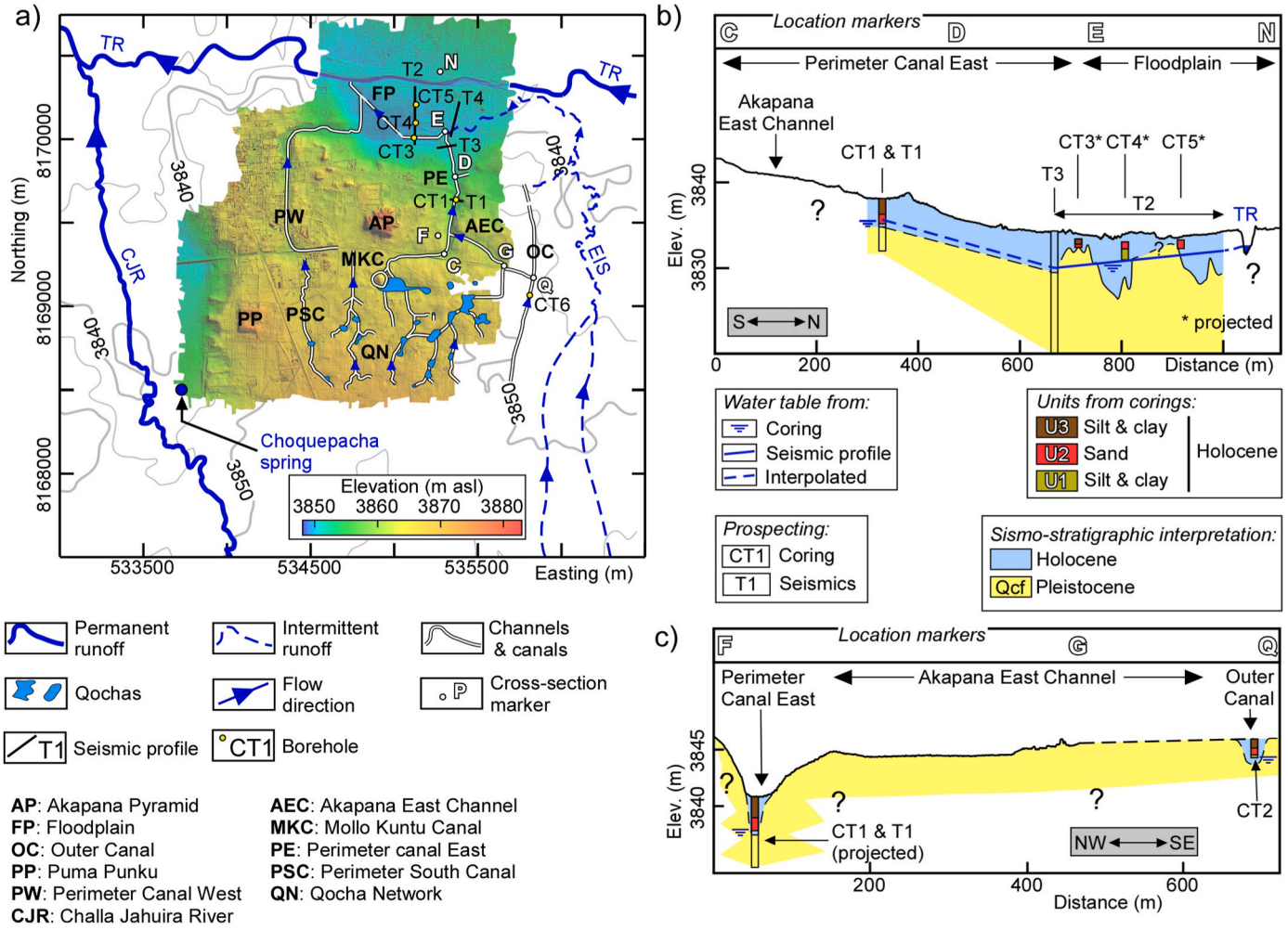

Fig. 7. Synthesis map and hydrostratigraphic results. a) Synthesis map of the main components of the Tiwanaku hydraulic network with their most probable water flow directions. b) South-North stratigraphic and hydrostratigraphic interpreted cross-section of the eastern arm of the perimeter canal illustrating the depth and slope of the water table interpolated from seismic profiling and borehole stratigraphy. c) East-West interpreted stratigraphic cross-section of the Akapana East Channel.

are synthesized in Fig. 7a and validate most of the water pathways proposed by archaeologists (Ortloff and Janusek (2016) and references herein).

Water flow directions obtained from the analysis of the high-resolution digital surface model indicate that the principal components of this hydraulic network are the eastern and western arms of the perimeter canal (PE and PW, respectively) which flow northward, in agreement with the general topographic slope of the site, and connect the South and North agro-pastoral areas. Only the southern part of the perimeter canal flows perpendicular to the general N–S slope (cross-section H-A-I-C in Fig. 2d) and is likely an engineered structure constructed to supply the canal from the adjacent qocha area, and possibly water derived from the CJR (not investigated because of the presence of modern constructions), and the southern edge of the Eastern Intermittent Stream (EIS). Hence, the topographical and lithological information suggest that the PE and PW were probably natural structures originating from badland-like geomorphology (Fig. 7a) that promoted gully erosion (Faulkner, 2008; Howard, 2009), and which could have been used by the first builders of the ceremonial centre (200 BCE to 200 CE) for the construction of their engineering hydraulic network. The perimeter canal was estimated to be at least ca. 30 m wide and 3 m deep (Fig. 3a and 4b) if considering a post-Tiwanaku sedimentary filling of at least 1 m (Fig. 5) for the PE. Such large dimensions suggest that the perimeter canal was probably used for the regulation of floods during the wet season as most of the intermittent tributaries such as the southern canals (PSC and MKC), the qocha channel network, and the eastern secondary canals (*i.e.* the Akapana East Channel, AEC, and the Outer Canal, OC) converge toward this latter. In addition, the proximity of the alluvial floodplain certainly accentuated the risks of canal overflow due to the backwater effect caused by the flow confluence action at the junction of the canal with the TR during flood events.

Surface topography, geophysical and lithological results suggest that, in contrast to the perimeter canal, the AEC and the OC (Fig. 7a) had much smaller dimensions (less than 10 m wide from the surface morphology analysis and an unknown but most probably reduced depth from EMI mapping) with lithological features (see section 4.3) supporting a less turbulent hydrodynamic regime typical of intermittent streams that were probably used to drain the civic space. It is worth mentioning that both the AEC and OC were probably connected to other intermittent streams in the East (*e.g.* EIS dashed lines in Fig. 7a) which remains difficult to assess because of the very smooth relief. Finally, the morphology of the alluvial plain (Fig. 7b) depicts laterally shifted incisions of the Qcf formation that can be related to historical changes in the course of the TR streambed as already shown for its downstream part (Vella and Loget, 2021). Such geomorphological features together with the lithological observation, do not support a permanent historical occupation of this area.

From the combination of seismic profiling and observations in boreholes, we characterized a water table dipping North below the monumental area (T1 in Fig. 7b), and with a hydraulic gradient of around 0.6 % (blue dashed line in Fig. 7b). This is in agreement with the slope of the present-day CJR in the study area (0.45 %), and the recent findings of Flores Avilés et al. (2020) in the Katari-Lago Menor basin aquifer (0.1 %). The hydraulic gradient observed between CT2 and CT1 (Fig. 7c) also supports a groundwater flow to the north in the southern part of the study site. All of these water table inclinations are consistent with the 3.5% hydraulic gradient reported for the underground sandstone channels that drained the monumental centre area to the North (Ortloff and Janusek, 2016).

The presence of the Choquepacha spring (~3839.5 m asl, Fig. 2a) (Janusek and Bowen, 2018), a resurgence of the aquifer located in the Pleistocene colluvio-fluvial formation (Qcf formation) (GEOBOL, 1995), attests to the presence of an outcropping water table in the South-West part of the site. In the PE, the water table was also identified at a shallow depth within the ancient canal bed (around 2.5 and 3 m deep in May 2015 and July 2015, respectively; Fig. 7c). To the North, in the alluvial floodplain (transect T2 in Fig. 7b), the water table is found oriented South with a hydraulic gradient of 0.15–0.3 %. It suggests that the TR drains into the water table in agreement with our observations made at the time of prospecting (dry season). Therefore, taken together, these data suggest that the southern area was mainly fed by the outcropping water table, whereas the canals were supplied at least intermittently by both the shallow water table and secondary tributaries of the Tiwanaku River (EIS and CJR).

In summary, the choice of this site by the former builders of the city of Tiwanaku testifies to an elaborate knowledge of the hydrology of the site and the management of water resources. It ensured water supply and flood management with the extreme intra- and inter-annual variability of precipitations in this area of the central Andes. The presence of an outcropping water table to the south should have enabled the monumental complex to be supplied with water at low water levels, particularly during the dry season. To the north, the proximity of the alluvial plain (which drains into the site's water table) also allowed for maintenance of the level of the water table within the canals, keeping them flowing during the dry season. Furthermore, the large dimensions of the perimeter canal illustrate the flood control and drainage capacity of the monumental centre (underground canals), and the permanent and intermittent tributaries during the wet season. Finally, the establishment of qochas and agricultural land upstream of the monumental centre should have ensured water reserves during the dry season, and acted as a retention area during the wet one.

5.2. *Canal sedimentation in a palaeoenvironmental and archaeological context*

To reconstruct the chronology of canal operation in line with the palaeoclimatic and hydrological context, the terrestrial boreholes collected in the Tiwanaku canals (CT1 to CT6) were compared to a recently published reconstruction of Lake Titicaca level variation (Guédron et al., 2023). A composite stratigraphy was established from the analysis of boreholes CT1 and CT2 collected in the eastern perimeter and outer canals, respectively (Fig. 5a) to document a continuous chronology of this main channel.

Fig. 8 shows the comparison of the composite channel sediment stratigraphy with the reconstruction of water-level variability in Lake Titicaca during the Late Holocene. It documents synchronous changes in sedimentation for the two records that can be inferred as hydrological changes in phase with the human occupation of the site and its possible re-organization. The older riverine sediment collected in the channel boreholes (Unit 1, before 200 BCE, Fig. 8a) corresponds chronologically to the Middle Formative period (800–200 BCE). The end of this period is characterized by a decrease in precipitation (Baker et al., 2009), a decline in the hydrological regime of the Altiplano rivers (Baucom and Rigsby, 1999; Rollins, 2001), and the downcutting of Rio Llave terrace sediment (Abbott et al., 1997) during a drier period when Lake Titicaca level dropped (Baker et al., 2001; Weide et al., 2017; Guédron et al., 2023).

Strikingly, the occurrence of the coarser red channel sediment in the Tiwanaku perimeter canal (Unit 2, between 200 BCE and 200 CE) coincides with a sharp lake rise reported ca. 200 BCE (Fig. 8b), suggesting that water was channelized during a period of increased precipitation in the Altiplano (Weide et al., 2017; Guédron et al., 2023). Such channelization of the perimeter canal also coincides with the construction of the civic spaces of Tiwanaku during the first century CE (Marsh et al., 2019), the beginning of the pre-urbanization of Tiwanaku (Janusek, 2004), and the development of raised field agriculture between 200 BCE and 500 CE (Bandy, 2013a). Hence, the channelling of water during this period of urban development was likely encouraged to protect the city against flooding and to maintain sufficient resources for the development of agriculture and the city.

Then, this coarse-grained red unit 2 is overlaid without gradation by a fine organic-rich deposit (Unit 3) dated before 700 CE. It suggests a

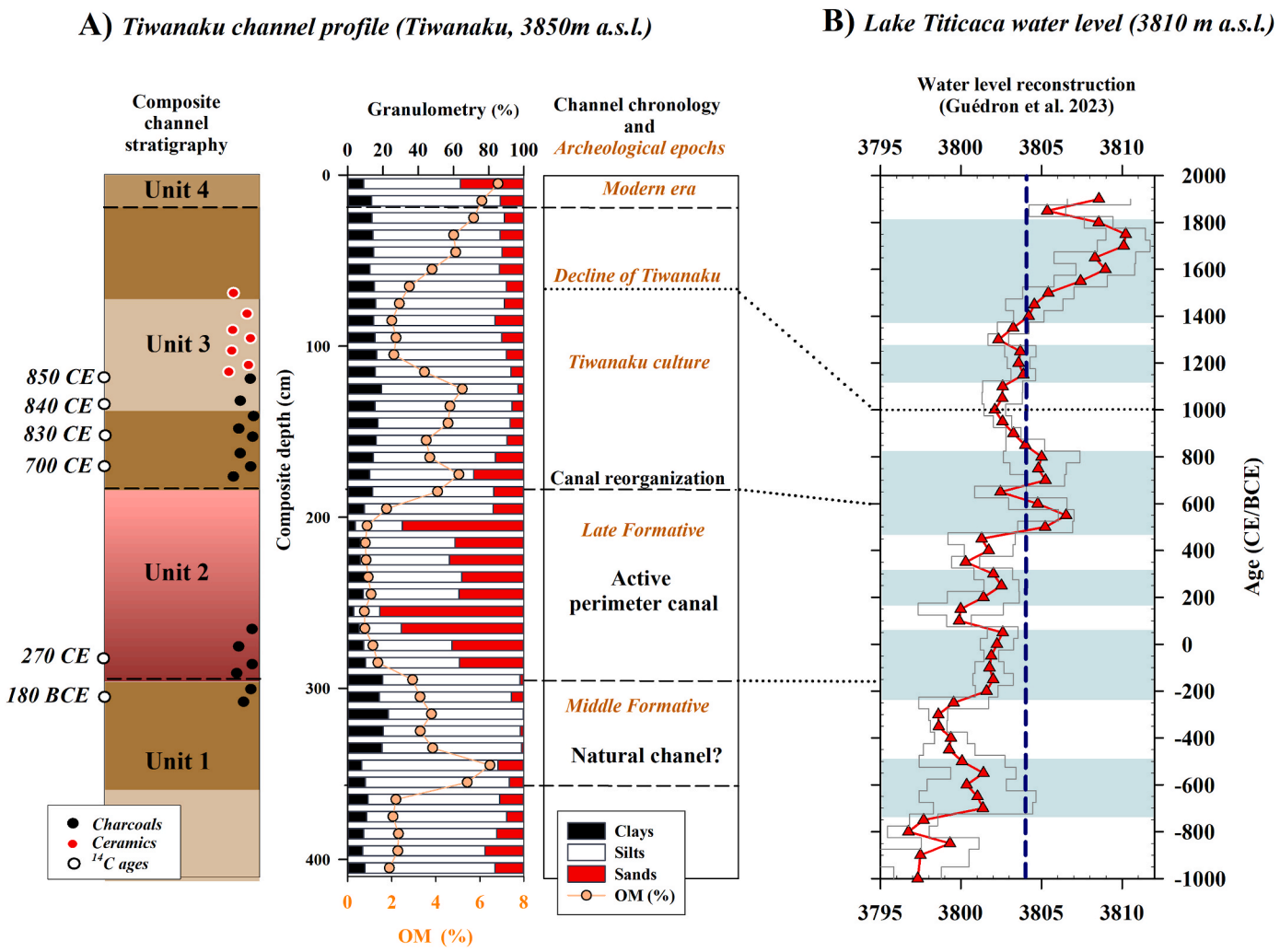

Fig. 8. a) Composite canal stratigraphy from 2 auger profiles collected in the perimeter canal (CT1; Units 2 to 4; 0–3 m) and in the outer canal (CT2; unit 1; 1.2–1.5 m). b) Lake Titicaca water-level reconstruction along the last past 3000 years (Guédron et al., 2023). The blue dotted line indicates the elevation of the modern overflow level (3804 m asl).

change from a turbulent canalized sedimentation to a slow water circulation allowing the sedimentation of eroded fine particles from the surrounding soils. This period, however, corresponds to another sharp rise in regional precipitation and a lake level rise between ca. 600 and 800 CE (Baker et al., 2009; Guédron et al., 2023). A rise in precipitation is not consistent with the change in canal sedimentation from high (coarse deposits in PC Unit 2) to low (fine deposits in PC Unit 2) velocity water circulation in the channel sediment. Hence, this change in sedimentation is likely attributed to a change in water management of the site during a wetter period. It could correspond to a remodelling of the channelization and possibly its partial abandonment, resulting in a change in the water routes and velocity.

Recent studies have proposed that the major lake-level rise at the end of the Formative Period (ca. 500 CE) inundated large shoreline areas and forced populations to migrate to higher elevations (Vella et al., 2017; Delaere and Guédron, 2022; Guédron et al., 2023). At that time, the technological, political and ritual development of the city of Tiwanaku certainly encouraged migration to this major regional political center (Kolata, 1993, 2003). Consistently, archaeologists have reported a rapid increase in population at Tiwanaku ca. 600 CE (Goldstein, 1993; Bandy, 2013b; Marsh et al., 2019) and the complete reorganization of the site including the enlargement of the monumental core (Akapana pyramid and the Kalassassaya platform) (Kolata, 2003; Janusek and Kolata, 2004; Vella et al., 2019), and the large-scale construction and use of raised field systems (Janusek and Kolata, 2004).

The scarcity of organic macro-remains in the top boreholes of Unit 2 did not allow precise dating of the beginning of these perturbations. In addition, the limited number of boreholes collected across the site does not allow us to conclude if such remodelling was performed at the entire or partial scale of the site and if the channel hydrological regime was uniformly perturbed. Archaeological excavations performed between 1988 and 1991 in the Akapana East sector (AKE-1M, AKE-1 and AKE-2; see Supplementary Information S-4) have, however, revealed the extension of domestic occupation in the external part of the perimeter canal (encompassing an area of 1 km^2) only after 600 CE. In contrast, during the LF period and the beginning of the Tiwanaku Period (ca. 600 CE), both the ceremonial and domestic occupations were concentrated within the area of the perimeter canal (Janusek, 1994, 2004). After ca. 800 CE, important urbanistic transformations of the ceremonial centre were also reported by archaeologists, including the dismantling and reconstruction of the Putuni complex (Couture and Sampeck, 2003) in a cultural context of expansion and consolidation of the Tiwanaku state (Delaere et al., 2019). Such change in the structural organization of the monumental site probably included a reorganization of both the agricultural and the residential sectors (Rivera Casanovas, 2003). The hydraulic network was probably also partly restructured, reducing the number of water sources that supplied the canal. This would thus explain the decrease in water hydrodynamics observed in the PE. The

extension of raised field agriculture during this epoch could also have contributed to such dissipation of the hydraulic energy in the canals. Indeed, the presence of the Unit 3 layer in the southern part of the alluvial plain (core CT3, Fig. 5) supports such extension of raised field agriculture before 850 CE (radiocarbon age at the bottom of Unit 3 in core CT3, Fig. 5) to the alluvial plain. It also supports the rise in elevation of the outlet part of the perimeter canal. Archaeological surveys revealed that wells were in use in the monumental core at that time (Janusek, 2003b). However, the perimeter canal may have still been in use as surveys reported domestic activities requiring water on the border of the PE (*i.e.* adobe construction, "chicha" (fermented drinks) and food production; see Supplementary Information S-4) (Janusek, 2003a) until the decline of the Tiwanaku culture ca. 1000 CE. In contrast, both the AEC and the OC were likely abandoned or subsumed during the expansion of the city as multiple Tiwanaku foundations of adobe construction were reported in this sector (Janusek, 2003a). Finally, at the decline of the Tiwanaku culture (ca. 1000 CE), the site and the canals were partially abandoned. This period corresponds to a significant decrease of the lake water level. The occupied space was significantly reduced but still maintained by societies mainly centred on pastoral activities (Altiplano artefacts found in TT1). The use of raised field systems declined precipitously after 1000 CE (Janusek and Kolata, 2004).

6. Conclusion

The combination of morphological, geophysical, geological and archaeological tools provides a quantitative assessment of Tiwanaku's hydrological network. A large U-shaped perimeter canal encircled and drained the monumental centre. It is confirmed that the inhabitants of the city of Tiwanaku constructed this complex web of artificial canals before the creation of the Tiwanaku state (ca. 600 CE). These canals most probably originate from existing natural channels and were used to channel water from the various local water sources and groundwater to supply both agricultural landscapes and the urban and ceremonial centres. In addition to this technical aspect of water management, the canal network probably had a major symbolic role at the cultural level, since it allowed, among other things, the delimitation of the residential sectors of ritual architecture.

The location and organization of the network testify to an advanced knowledge of the local hydrology by the former builders of the city. It was supplied by an outcropping water table and by secondary tributaries. It ensured water supply and flood management in relation to the extreme intra- and inter-annual variability of precipitations in this area of the central Andes.

The canal construction commenced during the early Late Formative Period (around 200 BCE to 300 CE) and continued to be used through the start of the Tiwanaku Period (ca. 600 CE). At that time, a major change in water management occurred, likely resulting from a major reorganization of the monumental centre during a period of wetter climate. This resulted in an adaptation of the hydraulic network reflecting the complex urban organization of the monumental core and the rise of agriculture during the Tiwanaku state. Further archaeological studies along the canal network will help increasing the chronological resolution of occupation and strengthen the links between the active/passive functioning of the canal and its anthropic use.

CRediT authorship contribution statement

Marc-Antoine Vella: Conceptualization, Formal analysis, Funding acquisition, Investigation, Methodology, Project administration, Resources, Supervision, Validation, Writing - original draft, Writing - review & editing. **Grégory Bièvre:** Conceptualization, Formal analysis, Investigation, Methodology, Resources, Writing - original draft. **Christophe Delaere:** Investigation, Methodology, Writing - original draft. **Julien Thiesson:** Formal analysis, Investigation, Resources, Writing - review & editing. **Roger Guérin:** Investigation, Methodology, Resources, Writing - review & editing. **Claudia Rivera-Casanovas:** Investigation, Writing - review & editing. **Stéphane Guédron:** Conceptualization, Methodology, Resources, Writing - original draft.

Declaration of competing interest

The authors declare that they have no known competing financial interests or personal relationships that could have appeared to influence the work reported in this paper.

Data availability

Data will be made available on request.

Acknowledgements

The authors thank the "Centro de Investigaciones Arqueológicas Antropológicas y de Administración de Tiwanaku-CIAAAT", Julio N. Condori Amaru (Director General Ejecutiovo del CIAAAT) and José Gallego Revilla for granting access to the Digital Surface Model. Corey Bowen (the University of Illinois at Chicago, USA) provided the coordinates of the Choquepacha spring. Gabriela Patricia Flores Avilés is acknowledged for fruitful discussions on the hydrogeological setting of the area. This study was funded by a grant from Institut Français d'Etudes Andines (IFEA) and the French Ministry of Foreign Affairs (M.-A.V.). The local communities are acknowledged for granting access to perform geophysical surveys and geological coring. Dr Kristen Cook (Univ. Grenoble Alpes) is acknowledged for helping with English writing. The authors thank the editor and two reviewers for their careful and constructive comments. G.B. and S.G. are part of LabEx OSUG@2020 (ANR10604 LABX56).

Appendix A. Supplementary data

Supplementary data to this article can be found online at https://doi.org/10.1016/j.quascirev.2023.108475.

References

Abbott, M.B., Binford, M.W., Brenner, M., Kelts, K.R., 1997. A 3500 ^{14}C yr high-resolution record of water-level changes in Lake Titicaca, Bolivia/Peru. Quat. Res. 47, 169–180.

Angelakis, A.N., Spyridakis, D.S., 2010. A brief history of water supply and wastewater management in ancient Greece. Water Supply 10, 618–628. https://doi.org/10.2166/ws.2010.105.

Avilés, Flores, G, P., Descloîtres, M., Duwig, C., Rossier, Y., Spadini, L., Legchenko, A., Soruco, A., Argollo, J., Pérez, M., Medinaceli, W., 2020. Insight into the Katari-Lago Menor Basin aquifer, Lake Titicaca-Bolivia, inferred from geophysical (TDEM), hydrogeological and geochemical data. J. S. Am. Earth Sci. 99, 102479 https://doi.org/10.1016/j.jsames.2019.102479.

Baker, P.A., Seltzer, G.O., Fritz, S.C., Dunbar, R.B., Grove, M.J., Tapia, P.M., Cross, S.L., Rowe, H.D., Broda, J.P., 2001. The history of South American tropical precipitation for the past 25,000 years. Science 291, 640–643. https://doi.org/10.1126/science.291.5504.640.

Baker, P.A., Fritz, S.C., Burns, S.J., Ekdahl, E., Rigsby, C.A., 2009. The nature and origin of decadal to millennial scale climate variability in the southern tropics of South America: the Holocene record of lago umayo, Peru. In: Vimeux, F., Sylvestre, F., Khodri, M. (Eds.), Past Climate Variability in South America and Surrounding Regions: from the LastGlacial Maximum to the Holocene. Springer. https://doi.org/10.1007/978-90-481-2672-9_13.

Bandy, M.S., 2005. Energetic efficiency and political expediency in Titicaca Basin raised field agriculture. J. Anthropol. Archaeol. 24, 271–296. https://doi.org/10.1016/j.jaa.2005.03.002.

Bandy, M.S., 2013a. Demographic dimensions of Tiwanaku urbanism. In: Vranich, A., Stanish, C. (Eds.), Advances in Titicaca Basin Archaeology. The Cotsen Institute of Archaeology, Los Angeles, CA, USA.

Bandy, M.S., 2013b. Tiwanaku origins and early development: the political and moral economy of a hospitality state. In: Vranich, A., Stanish, C. (Eds.), Visions of Tiwanaku. The Cotsen Institute of Archaeology, Los Angeles, CA, USA.

Baucom, P.C., Rigsby, C.A., 1999. Climate and lake-level history of the northern Altiplano, Bolivia, as recorded in Holocene sediments of the Rio Desaguadero. J. Sediment. Res. 69, 597–611.

Browman, D.L., 1981. New Light on Andean Tiwanaku: a detailed reconstruction of Tiwanaku's early commercial and religious empire illuminates the processes by which states evolve. Am. Sci. 69, 408–419.
Couture, N.C., Sampeck, K., 2003. Putuni: history of palace architecture at Tiwanaku. In: Kolata, A.L. (Ed.), Tiwanaku and its Hinterland, Archaeology and Paleoecology of an Andean Civilization, Urban and Rural Archaeology, vol. 2. Smithsonian Institution Press, Washington DC, USA.
Dejoux, C., Iltis, A. (Eds.), 1992. Lake Titicaca: a Synthesis of Limnological Knowledge. Kluwer Academic Publishers, Dordrecht, Netherlands.
Delaere, C., 2017. The location of Lake Titicaca's coastal area during the Tiwanaku and inca periods: methodology and strategies of underwater archaeology. J. Marit. Archaeol. 12, 223–238. https://doi.org/10.1007/s11457-017-9187-6.
Delaere, C., Guédron, S., 2022. The altitude of the depths: use of inland water archaeology for the reconstruction of inundated cultural landscapes in Lake Titicaca. World Archaeol. 54, 67–83. https://doi.org/10.1080/00438243.2022.2077827.
Delaere, C., Capriles, J.M., Stanish, C., 2019. Underwater ritual offerings in the Island of the Sun and the formation of the Tiwanaku state. Proc. Natl. Acad. Sci. USA 116, 8233–8238. https://doi.org/10.1073/pnas.1820749116.
Delaere, C., Guédron, S., Fritz, S.C., 2023. Interactions between past societies and environmental change in the Lake Titicaca region (tropical Andes). Past Global Changes Magazine 31, 18–19. https://doi.org/10.22498/pages.31.1.18.
Di Stefano, C., Ferro, V., Mirabile, S., 2011. Testing the grain-size distribution determined by Laser diffractometry for Sicilian soils. Journal of Agricultural Engineering 42, 39–48.
Erickson, C.L., 1992. Prehistoric landscape management in the Andean highlands: raised field agriculture and its environmental impact. Popul. Environ. 13, 285–300. https://doi.org/10.1007/bf01271028.
Erickson, C., 2000. The Lake Titicaca basin: a Precolumbian built landscape. In: Lentz, D. (Ed.), Imperfect Balance: Landscape Transformations in the Precolumbian Americas. Columbia University Press, New York, USA.
Faulkner, H., 2008. Connectivity as a crucial determinant of badland morphology and evolution. Geomorphology 100, 91–103. https://doi.org/10.1016/j.geomorph.2007.04.039.
Fritz, S.C., Baker, P.A., Tapia, P., Garland, J., 2006. Spatial and temporal variation in cores from Lake Titicaca, Bolivia/Peru during the last 13,000 yrs. Quat. Int. 158, 23–29.
Gallego-Revilla, J.I., Pérez-González, M.E., 2018. Tiwanaku, entre el cielo y la tierra. UNESCO office, Quito, Ecuador.
GEOBOL, 1995. Tiahanacu; La Paz; jesús de Machaca; calamarca. In: *Geological sheet escala 1:100000*, Servicio Geologico de Bolivia (GEOBOL) and Geological Swedish (AB).
Goldstein, P., 1993. Tiwanaku temples and state expansion: a Tiwanaku sunken-court temple in Moquegua, Peru. Lat. Am. Antiq. 4, 22–47.
Guédron, S., Delaere, C., Fritz, S.C., Tolu, J., Sabatier, P., Devel, A.-L., Heredia, C., Vérin, C., Alves, E.Q., Baker, P.A., 2023. Holocene variations in Lake Titicaca water level and their implications for sociopolitical developments in the central Andes. Proc. Natl. Acad. Sci. USA 120. https://doi.org/10.1073/pnas.2215882120.
Heiri, O., Lotter, A.F., Lemcke, G., 2001. Loss on ignition as a method for estimating organic and carbonate content in sediments: reproducibility and comparability of results. J. Paleolimnol. 25, 101–110. https://doi.org/10.1023/a:1008119611481.
Hogg, A.G., Heaton, T.J., Hua, Q., Palmer, J.G., Turney, C.S., Southon, J., Bayliss, A., Blackwell, P.G., Boswijk, G., Ramsey, C.B., Pearson, C., Petchey, F., Reimer, P., Reimer, R., Wacker, L., 2020. SHCal20 southern Hemisphere calibration, 0–55,000 Years cal BP. Radiocarbon 62, 759–778. https://doi.org/10.1017/RDC.2020.59.
Howard, A.D., 2009. Badlands and gullying. In: Parsons, A.J., Abrahams, A.D. (Eds.), Geomorphology of Desert Environments. Springer. https://doi.org/10.1007/978-1-4020-5719-9-10.
Hua, Q., Barbetti, M., Rakowski, A.Z., 2013. Atmospheric radiocarbon for the period 1950-2010. Radiocarbon 55, 2059–2072.
Janusek, J.W., 1994. State and Local Power in a Prehispanic Andean Polity: Changing Patterns of Urban Residence in Tiwanaku and Lukurmata. University of Chicago, Bolivia. USA.
Janusek, J.W., 2003a. The changing face of Tiwanaku residential life: state and local identity in an Andean city. In: Kolata, A.L. (Ed.), Tiwanaku and its Hinterland: Archaeology and Paleoecology of an Andean Civilization. Smithsonian Institution Press, Washington DC, USA.
Janusek, J.W., 2003b. Vessels, time, and society: toward a ceramic chronology in the Tiwanaku heartland. In: Kolata, A.L. (Ed.), Tiwanaku and its Hinterland: Archaeology and Paleoecology of an Andean Civilization. Smithsonian Institution Press, Washington DC, USA.
Janusek, J.W., 2004. Identity and Power in the Ancient Andes: Tiwanaku Cities through Time. Routledge, Oxon, UK.
Janusek, J.W., Bowen, C., 2018. Tiwanaku as telluric waterscape. Water and stone in a highland Andean city. In: Jennings, J., Swenson, E.R. (Eds.), Powerful Places in the Ancient Andes. University of New Mexico Press, Albuquerque, USA.
Janusek, J.W., Kolata, A.L., 2004. Top-down or bottom-up: rural settlement and raised field agriculture in the Lake Titicaca Basin, Bolivia. J. Anthropol. Archaeol. 23, 404–430. https://doi.org/10.1016/j.jaa.2004.08.001.
Kolata, A.L., 1993. The Tiwanaku: Portrait of an Andean Civilization. Blackwell, Cambridge, UK.
Kolata, A.L., 2003. The social production of Tiwanaku: political economy and authority in a native Andean state. In: Kolata, A.L. (Ed.), Tiwanaku and its Hinterland: Archaeology and Paleoecology of an Andean Civilization. Smithsonian Institution Press, Washington DC, USA.
Kolata, A.L., Ortloff, C.R., 1989. Thermal analysis of Tiwanaku raised field systems in the Lake Titicaca Basin of Bolivia. J. Archaeol. Sci. 16, 233–263. https://doi.org/10.1016/0305-4403(89)90004-6.
Kolata, A.L., Ortloff, C.R., 1996. Tiwanaku raised-field agriculture in the Lake Titicaca Basin of Bolivia. In: Kolata, A.L. (Ed.), Tiwanaku and its Hinterland: Archaeology and Paleoecology of an Andean Civilization. Smithsonian Institution Press, Washington DC, USA.
Lasaponara, R., Masini, N., 2014. Beyond modern landscape features: new insights in the archaeological area of Tiwanaku in Bolivia from satellite data. Int. J. Appl. Earth Obs. Geoinf. 26, 464–471. https://doi.org/10.1016/j.jag.2013.09.006.
Marsh, E.J., Roddick, A.P., Bruno, M.C., Smith, S.C., Janusek, J.W., Hastorf, C.A., 2019. Temporal inflection points in decorated pottery: a bayesian refinement of the late formative chronology in the southern Lake Titicaca basin, Bolivia. Lat. Am. Antiq. 30, 798–817. https://doi.org/10.1017/laq.2019.73.
Marty, P., Darras, L., Tabbagh, J., Benech, C., Simon, F.-X., Thiesson, J., 2015. WuMapPy open source s/w for geophysical survey data processing. In: 11th International Conference on Archaeological Prospection. 15-19 September, Warsaw, Poland.
Mourguiart, P., Corrège, T., Wirrmann, D., Argollo, J., Montenegro, M., Pourchet, M., Carbonel, P., 1998. Holocene palaeohydrology of Lake Titicaca estimated from an ostracod-based transfer function. Palaeogeogr. Palaeoclimatol. Palaeoecol. 143, 51–72. https://doi.org/10.1016/S0031-0182(98)00068-6.
Ortloff, C.R., 2009. Water Engineering in the Ancient World: Archaeological and Climate Perspectives on Societies of Ancient South America, the Middle East, and South-East Asia. Oxford University Press, Oxford, England.
Ortloff, C.R., Janusek, J.W., 2016. Hydrologic engineering of the Tiwanaku. In: Seline, H. (Ed.), Encyclopaedia of the History of Science, Technology and Medicine in Non-western Cultures. Springer.
Pérez González, M.E., Gallego Revilla, J.I., 2020. A new environmental and spatial approach to the Tiwanaku World Heritage site (Bolivia) using remote sensing (UAV and satellite images). Geoarchaeology 35, 416–429. https://doi.org/10.1002/gea.21778.
Pix4D SA, 2016. Pix4D Mapper. Prilly, Switzerland. https://www.pix4d.com.
Ponce Sanginés, C., 1972. Tiwanaku: espacio, tiempo y cultura; ensayo de síntesis arqueológica. AcademiaNacional de Ciencias de Bolivia, La Paz, Bolivia.
Posnansky, A., 1945. Tihuanacu: the Cradle of American Man. JJ Augustin, New York, USA.
Purdue, L., 2015. Construction, maintenance and abandonment of hydraulic systems: hydroclimatic or social constraints? A case study of prehistoric Hohokam irrigation systems (Phoenix, Arizona, USA). Water History 7, 73–99. https://doi.org/10.1007/s12685-014-0121-7.
Rivera Casanovas, C., 2003. Ch'iji Jawira: a case of ceramic specialization in the Tiwanaku urban periphery. In: Kolata, A.L. (Ed.), Tiwanaku and its Hinterland: Archaeology and Paleoecology of an Andean Civilization. Smithsonian Institution Press, Washington DC, USA.
Rollins, S.M., 2001. Quaternary Lacustrine and Fluvial History of the Central Bolivian Altiplano as Recorded in Subsurface Strata of the Rio Desaguadero Valley. Bolivia.
Rücker, C., Günther, T., Wagner, F.M., 2017. pyGIMLi: an open-source library for modelling and inversion in geophysics. Comput. Geosci. 109, 106–123. https://doi.org/10.1016/j.cageo.2017.07.011.
Sharma, P.V., 1997. Environmental and Engineering Geophysics. Cambridge University Press, Cambridge, UK.
Stanish, C., 2003. Ancient Titicaca: the Evolution of Complex Society in Southern Peru and Northern Bolivia. University of California Press, CA, USA.
Storozum, M., Liu, H., Qin, Z., Ming, K., Fu, K., Wang, H., Kidder, T., 2018. Early evidence of irrigation technology in the North China plain: geoarchaeological investigations at the anshang site, neihuang county, henan province, China. Geoarchaeology 33, 143–161. https://doi.org/10.1002/gea.21634.
Sutherland, A.J., 1967. Proposed mechanism for sediment entrainment by turbulent flows. J. Geophys. Res. 72, 6183–6194. https://doi.org/10.1029/JZ072i024p06183.
Tarboton, D.G., 1997. A new method for the determination of flow directions and upslope areas in grid digital elevation models. Water Resour. Res. 33, 309–319. https://doi.org/10.1029/96WR03137.
Telford, W.M., Geldart, L.P., Sheriff, R.E., 1990. Applied Geophysics. Cambridge University Press, Cambridge, UK.
Vella, M.-A., Loget, N., 2021. Geomorphological map of the Tiwanaku River watershed in Bolivia: implications for past and present human occupation. Catena 206, 105508. https://doi.org/10.1016/j.catena.2021.105508.
Vella, M.-A., Sejas, S., Lucero Mamani, K., Rodriguez, L.A., Rivera Casanovas, C., Guedron, S., Brisset, E., Bievre, G., Menacho Cespedes, J., Argollo, J., Escobar, K., Ortuño, T., 2017. La misión Franco-Boliviana Paleoambiente y Arqueología del Río Guaquira-Tiwanaku (Bolivia): un estudio multidisciplinario de las interacciones entre las Sociedades Antiguas y el Medioambiente. Bulletin de l'Institut français d'études andines 47 (2), 169–193.
Vella, M.-A., Ernenwein, E., Janusek, J., Koons, M., Thiesson, J., Sanchez, C., Guérin, R., Camerlynck, C., 2019. New insights into prehispanic urban organization at Tiwanaku (NE Bolivia): cross combined approach of photogrammetry, magnetic surveys and previous archaeological excavations. J. Archaeol. Sci.: Report 23, 464–477. https://doi.org/10.1016/j.jasrep.2018.09.023.
Vranich, A., Stanish, C. (Eds.), 2013. Visions of Tiwanaku. The Cotsen Institute of Archaeology, Los Angeles, CA, USA.
Weide, D.M., Fritz, S.C., Hastorf, C.A., Bruno, M.C., Baker, P.A., Guédron, S., Salenbien, W., 2017. A ~6000 yr diatom record of mid- to late Holocene fluctuations in the level of Lago Wiñaymarca, Lake Titicaca (Peru/Bolivia). Quat. Res. 88, 179–192. https://doi.org/10.1017/qua.2017.49.
Wilkinson, T.J., Philip, G., Bradbury, J., Dunford, R., Donoghue, D., Galiatsatos, N., Lawrence, D., Ricci, A., Smith, S.L., 2014. Contextualizing early urbanization:

settlement cores, early states and agro-pastoral strategies in the fertile crescent during the fourth and third millennia BC. J. World PreHistory 27, 43–109. https://doi.org/10.1007/s10963-014-9072-2.

Wittfogel, K.A., 2017. The structure of political geography. In: Kasperson, R.E., Minghi, J.V. (Eds.), The Structure of Political Geography. Routledge, New York, USA. https://doi.org/10.4324/9781315135267.

Yevjevich, V., 1992. Water and civilization. Water Int. 17, 163–171. https://doi.org/10.1080/02508069208686135.